



Self-restoration of Underwater Low Adhesive Superoleophobicity on Shape Memory Polymer Arrays

Dongjie Zhang,^{1,2} Xinyu Wang,¹ Yaoxu He,¹ Yujie Feng,² Zhongjun Cheng,^{1,*} Yingbin Song,¹ Dongdong Hu¹ and Yuyan Liu^{1,*}

Abstract

Self-restoration property is a good candidate to prepare stable underwater superoleophobicity. However, almost all existing research interest focus on surface superhydrophobicity in air. Herein, a new underwater superoleophobic low adhesion surface with self-healing capacity is reported through constructing a hierarchical micro/nanostructure on epoxy shape memory polymer (ESMP) and modifying (3-Aminopropyl) triethoxysilane (APTES). After a simple heating process, the crushed surface microstructure and low adhesive superoleophobicity which are damaged under external pressure can be recovered spontaneously, indicating that the prepared surface has great self-healing properties. The self-healing property can be attributed to the excellent shape memory effect of ESMP and the good hydrophilicity of APTES. Finally, the obtained surface is further used as a rewritable platform in the storage and transportation of oil droplets in water. This work introduces the wetting control of ESMP into water media, which extends the application range of ESMP and opens up some new viewpoints in constructing underwater self-healing superoleophobic surfaces.

Keywords: Self-restoration; Low adhesion; Underwater superoleophobicity; Shape memory polymer; Microstructure.

Received: 10 August 2021; Revised: 27 September 2021; Accepted: 01 October 2021.

Article type: Research article.

1. Introduction

In the past decades, underwater superoleophobic surfaces have drawn considerable attention since they have huge promising applications in various fields,^[1-4] including oil-water/emulsion separation,^[5,6] antifouling of underwater devices,^[7,8] drag reduction,^[9] and so on. To get the superoleophobicity in water, hierarchical microstructure^[10] is usually used to capture water and form a water layer, which is favorable for resisting the contact between substrates and oil droplets and forming oil-repellent properties. Up to now, underwater superoleophobic surfaces with various kinds of microstructures have been reported, such as hierarchical cylinder arrays,^[11] lotus-leaf-like micro/nanostructures prepared from electrospraying, electrospinning,^[12] *etc.* However, almost all these surface microstructures are prone to be damaged in the realistic

application,^[13,14] finally leading to the loss of the underwater superoleophobicity and corresponding functions.

To solve the above-mentioned problem, and inspired by the self-healing properties of natural plants,^[15,16] robust and durable super-wetting surfaces^[17-20] with self-healing properties bring us new hopes. Lots of such self-healing super-wetting surfaces^[21-23] have been reported in recent years. For example, by injecting the low surface energy agents into the rough porous matrix, the damage caused by plasma damage, machine washing, or abrasion can be healed by the self-diffusion process of the trapped healing agents.^[24-27] Besides, regenerating topographic structures is also an important strategy to construct self-restoration super wetting surfaces.^[28] Nevertheless, almost all reported self-healing surfaces are focused on the recovery of superhydrophobicity in air. Achieving similar self-healing functions on other super wetting phenomena, such as underwater superoleophobicity in water, is still extremely rare. Recently, Zhou^[29] *et al.* tried to solve this problem and prepared a seawater-induced self-healing underwater superoleophobic coating relying on the self-polishing polymer and seawater-responsive polymer-grafted SiO₂ nanoparticles. However, the healed micromorphology was not the original micromorphology, and the self-healing property was due to the exposure of the self

¹ State Key Laboratory of Urban Water Resource and Environment, School of Chemistry and Chemical Engineering, Harbin Institute of Technology, Harbin 150001, China.

² State Key Laboratory of Urban Water Resource and Environment, School of Environment, Harbin Institute of Technology, No 73 Huanghe Road, Harbin, Heilongjiang, 150090, China.

*E-mail: chengzhongjun@iccas.ac.cn (Z. Cheng);

liuyy@hit.edu.cn (Y. Liu)

similar structure of the bulk to the top surface. It is reasonable to believe that when the bulk substrates are exhausted, the restoration of the underwater superoleophobicity will be difficult. Besides, Wu^[30] *et al.* fabricated an underwater superoleophobic surface composed of hydrophilic polymeric chain-modified hierarchical microgel spheres, and the swell of microgel spheres together with the replenishment of hydrophilic chains could lead to regeneration of the underwater superoleophobicity as the coating is mechanically destroyed. Nevertheless, the strategy relied on a particular hydrophilic polymer and microgel, which is hard to be extended. In this regard, advancing a new strategy to design self-healing underwater superoleophobic surfaces is still highly desired.

In this work, we report a new strategy and demonstrate a self-healing underwater superoleophobic surface through modifying (3-Aminopropyl) triethoxysilane (APTES) on epoxy shape memory polymer (ESMP) arrays. The as-prepared surface shows low adhesive underwater superoleophobicity. Under external pressure, the surface microstructure will be collapsed, leading to the loss of low adhesive properties. As a result, the surface is converted into high adhesive superoleophobicity in water. After a simple heating process, the crushed surface microstructure and related low adhesive superoleophobic performance will be recovered spontaneously. The excellent restorability can be ascribed to the combined effect of the good shape memory property of the polymer and the stable hydrophilicity of the surface chemistry. Moreover, based on the tunable adhesion during the self-healing process, the samples prepared in this work are applied in programmable storage and transportation of oil droplets in water. Although shape memory polymers (SMPs) have been broadly used in the control of surface wettability,^[31-34] and demonstrated many important applications in droplets storage,^[35] transportation,^[36-38] controllable bouncing,^[39] and self-restoration,^[40,41] *etc.*, all these works are concentrated on the water wetting performance in air, and applying the SMPs to regulate surface wetting performance and endowing the surface with a new function such as the self-healing property in water have never been reported.

2. Experimental section

2.1 Preparation of APTES-modified shape memory arrays

The shape memory arrays were first fabricated by the molding method according to our previous work (Fig. S1).^[42] Then the obtained ESMP samples were exposed to an O₂ plasma atmosphere for about 20 s to introduce hydroxyl groups, which can react with (3-Aminopropyl) triethoxysilane (APTES, 98%, Aldrich). Then, they were dealt with 95% ethanol (containing 5% deionized water) with 5% v/v APTES and a certain amount of glacial acetic acid (adjusting the solution pH to 5.5) at room temperature for about 4 hours. Ultimately, the samples were acquired followed by heating them in an oven at 90 °C for half an hour (Fig. S1b).

2.2 The self-repairing method of surface microstructure

To demonstrate the self-repairing ability of surface microstructure and underwater superoleophobicity, the pressing/recovery process was employed. Firstly, to simulate the damage to the microstructure, the samples were pressed under a certain pressure (≈ 2 MPa), as shown in Fig. S2. After that, the samples were heated at a different temperature to investigate the self-healing ability in both microstructure and wetting performance.

2.3 Characterization

Field-emission scanning electron microscope (SEM) apparatus (HITACHI, SU8010) and atomic force microscope (AFM, Bruker, Dimension Icon) were used to measure the surface morphologies. The contact angle measure meter (JC 2000D5, Shanghai Zhongchen Digital Technology Apparatus Co., Ltd) was employed to test water contact angles (CA) and sliding angles (SA). A confocal microscope (Olympus, OLS4100) was used to measure the 3D microstructure and corresponding profile curves.

3. Results and discussion

The ESMP pillars are fabricated by curing the mixture of diglycidyl ether of bisphenol (DGEBA), n-octylamine (OA), and m-xylylene diamine (MXDA) in polydimethylsiloxane (PDMS) template (Fig. S1a, Scheme S1). As shown in Fig. S3, the obtained ESMP surfaces are covered by irregular pillars with a cube shape, whose diameter and height are approximately 10 μm , and 10 μm and the pillars' spaces are 5 μm , 10 μm , 20 μm , and 30 μm , respectively. Meanwhile, one can see that the roughness on the top of the pillar is about 60.80 nm from the test of AFM (Fig. S4), and ESMP surfaces present hierarchical micro/nanostructure, which is in favor of constructing super wetting surfaces.^[43] However, the obtained surfaces display superhydrophobicity in the air (Fig. S5a, which matches previous work about the research of pure ESMP^[42] and SiO₂ modified SMP^[32] in the air) and superoleophilicity (1,2-dichloromethane droplet is used as an example) in water due to the relatively low surface energy of ESMP intrinsic property (Fig. S5b). To gain the underwater superoleophobic property, hierarchical micro/nano-structured surfaces are further modified by APTES. As a result of a modification, the Si element (characteristic peak of APTES) appears on the whole X-ray photoelectron spectroscopy (XPS) spectrum (Fig. S6). To learn the modification effect on micromorphology, the smooth ESMP surface is dealt with via the same method, resulting in a bit of increase of surface roughness from 0.56 nm to 2.80 nm (shown in AFM results in Fig. S7). Besides, via the test of Variable Angle Spectroscopic Ellipsometric, we can learn that the average thickness of APTES is about 4.35 nm. Together with the above-mentioned results, we can see that the surfaces are modified by APTES successfully. Importantly, as shown in Fig. 1a and Fig. S8, the surface micromorphology keeps constant after modification (the roughness on the top of the pillar is about 64.5 nm, Fig.

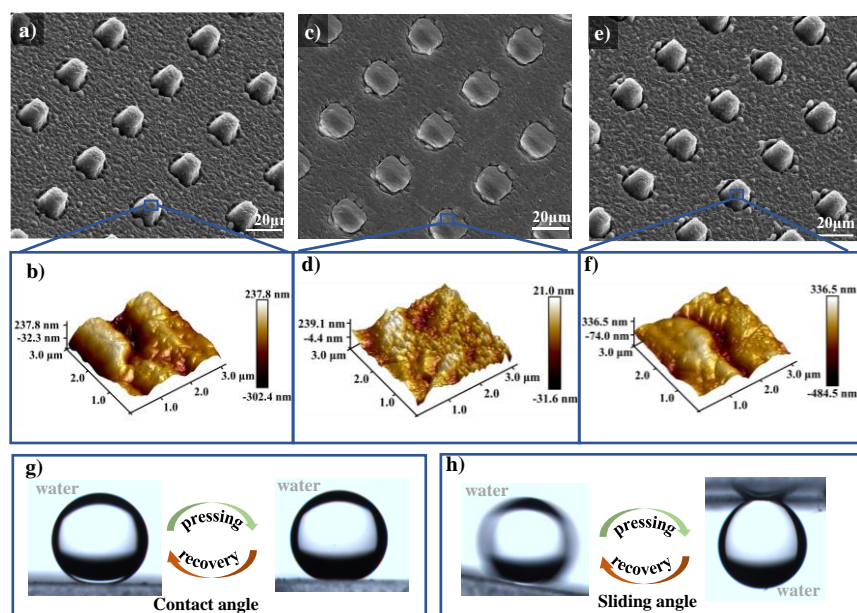


Fig. 1 SEM and AFM images of ESMP surface modified by APTES in a) and b) upright states, c) and d) collapsed states, e) and f) recovery states. From the shape change process, one can see that the as-prepared samples still have excellent shape memory effects both in micro and nanostructure. g) and h) are 1,2-dichloromethane's CAs and SAs on ESMP surfaces modified by APTES, indicating that reversible change between low and high adhesive underwater superoleophobicity and the excellent self-healing ability of the surfaces can be achieved.

1b). What's more, through wettability tests, we can see that SA is decreased following the increase of pillars' space, and 30 μm is the proper pillars' space in this work (Fig. S9) to obtain underwater superoleophobicity with low adhesive property (left in Figs. 1g and 1h), whose CA and SA (for 1,2-dichloromethane droplet) are about 160° and 8° , respectively. To demonstrate the self-healing ability, the surface is pressed. As shown in Fig 1c, the cube shapes are turned into pie shapes after pressing. At the same time, the tip surface roughness decreases to about 4.47 nm (Fig. 1d). Accordingly, wettability on the surface is also altered following the destruction of the micro/nanomorphology. As shown in the right images of Fig. 1g and Fig. 1h, the CA and SA on the collapsed surface are 158° and 180° , which means that the deformed surface lost its low adhesive property notwithstanding keeping the underwater superoleophobicity. Fortunately, all collapsed pillars can be recovered to an upright state (Fig. 1e) after being heated to a temperature higher than the glass transition temperature (T_g) of ESMP (T_g of ESMP modified by APTES is about 69.9°C , shown in Fig. S10). From Fig. 1f, one can also see the roughness of the pillar's top is recovered into 66.60 nm, demonstrating that the micro/nano structures come back to their original state. Finally, through the wettability test, the underwater superoleophobicity with low adhesion is also recovered following the recovery of micromorphology, meaning that surfaces prepared in this work have an excellent self-healing property. It should be noted that similar microstructure recovery has been demonstrated on our previously reported shape memory surface, however, it is concentrated on the restoration of superhydrophobicity in air.^[40] Realize the self-restoration of underwater

superoleophobicity by the polymer's shape memory effect has never been reported.

As above mentioned, the damage of micromorphology will lead to the loss of the low adhesive property of oil droplets in water, which means that researching the microstructure variation is necessary for a better understanding of the self-healing property. Therefore, we quantitatively test the microstructure change with a confocal laser scanning microscope (CLSM). Figs. 2a-b are the 3D CLSM image and corresponding profile of original ESMP pillars modified by APTES, exhibiting a similar morphology with SEM images (Fig. 1a). Through the calculation, one can see that the average height of pillars is about $9.8\ \mu\text{m}$, which is almost same with ESMP pillars without any modification (Fig. S11). Afterward, the surfaces are pressed by the external force, as a result, all the pillars are planished and the average height of pillars is decreased to $1.4\ \mu\text{m}$ (Figs. 2c and 2d). Then through a simple heating process, recovered to the original state (Figs. 2e and 2f) based

on the shape memory effect of ESMP substrate. Furthermore, the shape recovery can happen in various temperatures (higher than T_g) and the recovery time had a positive correlation with the temperature employed. As shown in Fig. 2g, when a low temperature (80°C) is utilized, about 90 s is necessary to make the total shape restoration; while under a relatively higher temperature (110°C), the recovery time will be sharply decreased to 18 s. Meanwhile, as displayed in Fig. 2h, when the temperature is fixed at 80°C , a series of pillars' heights and oil droplets sliding angles in water will be obtained by controlling the recovery time, meaning that a series of surfaces with different oil droplets adhesion in

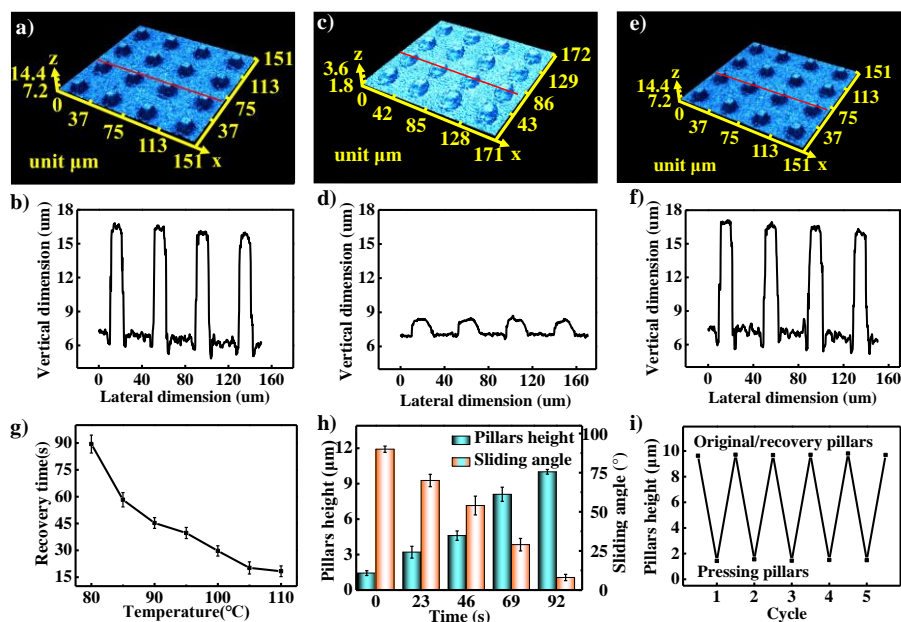


Fig. 2 3D morphology and corresponding outlines from Confocal Laser Scanning Microscope test for ESMP micro-structured surfaces with a) and b) upright pillars, c) and d) collapsed pillars, e) and f) recovery pillars. As shown in the images, the average pillars’ height can change to the original value after self-healing by heating. g) Statistic of recovery time at different temperatures. h) The change of average pillars’ height and underwater sliding angles of oil droplets following the change of recovery time at 80 °C. i) Statistic of average pillars’ height in several repeated pressing/recovery processes.

water could be obtained following the self-healing process. Moreover, the process of shape change can be reversibly repeated without any damage to morphology and change of size.

Furthermore, besides 1, 2- dichloromethane, a range of oil droplets (whose density is lighter and heavier than water) are employed to test the surfaces self-healing property, containing cyclohexane (CH), hexane (HA), petroleum ether (PE), toluene (TE), n-heptane (NH), carbon tetrachloride (CT), and dichloroethane (DE). Firstly, as displayed in Fig. 3a, all droplets have low sliding angles in water media on original surfaces. Then as the pillars collapsed, the oil droplets keep high contacts angles (Fig. S12) but can’t roll anymore (Fig. 3a). After being heated, all oil droplets can roll with low

sliding angles again similar to 1,2- dichloromethane, meaning the recovery of underwater superoleophobicity with the low adhesive property. Importantly, taking the wettability change of the n-hexane droplet as an example, the reversible transition between the rolling state and pinning state can remain after several cycles (Fig. 3b), meaning that the obtained surface has good stability.

In this work, the as-prepared surfaces have excellent self-healing properties of underwater superoleophobicity with low adhesion, which is ascribed to the shape memory effect of ESMP. The ESMP employed in this work is a kind of thermo-responsive material, which has two structural composites, one part is shape memory transition (or reversible thermal transition) guaranteeing the fixing and recovery of temporary

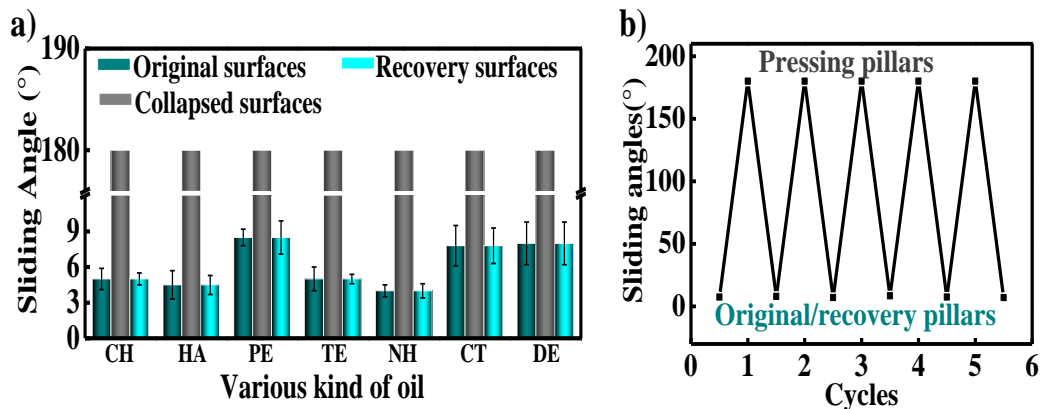


Fig. 3 a) Statistic of SAs of various oil droplets on surfaces with originally upright pillars, collapsed pillars, and recovery upright pillars in water media (the cyclohexane, hexane, petroleum ether, toluene, n-heptane, carbon tetrachloride, and dichloroethane were marked by CH, HA, PE, TE, NH, CT, and DE in the figure), meaning that the prepared samples with self-healing property are universal regardless of oil type. b) The variation of sliding angles in the consecutive processes of pressing and recovery.

shape; another part is a cross-linking network (including both physical cross-linking from the tail-to-tail entanglement of alkyl chains and chemical cross-linking from the reaction of epoxy groups and amidogen groups) using for setting the permanent shape.^[44,45] Meanwhile, the obtained ESMP has good flexibility (Fig. S13), apparent thermal reversible phase transition ability (displayed in Fig. S10), and notable shape memory effect with a shape recovery ratio of 98% and a shape fixed ratio of 99% (Fig. S14). The ability to memorize the temporary shape and recover the permanent shape makes it possible to exhibit various microstructure shapes and wettabilities in water. On obtained surfaces, the upright pillars with hierarchical microstructure are permanent shapes (bottom picture in Fig. 4a) and the molecular chains adopt conformations with the highest entropy (above picture in Fig. 4a), which is in a thermodynamically stable state. Meantime, after modification of APTES, the flat ESMP substrates show a clear increase in hydrophilicity and underwater oleophobicity (Figs. S15, S16 in supporting information). On surfaces with upright hydrophilic pillars, the spaces between pillars can be filled with water, forming a water layer between the oil droplets and surfaces. Therefore, the oil droplets on the ESMP pillared surfaces exhibit the Cassie state^[46] in water, and the surface shows underwater superoleophobicity with low adhesive properties (Fig. 4e).

After being pressed by an external force, the polymer chain conformations are changed and the pillars are collapsed (Fig. 4b). During that process, the chemical and physical crosslinking network can effectively protect the long-range chain from slipping, leading to the trap of entropy energy,^[44] which is the foundation of shape recovery. Besides, from the XPS result in Fig. S17 and Table S1, one can see that surface chemical composition will not change after being pressed by an external force, meaning that the surface still has hydrophilicity. However, due to the pillars' collapse, the surface wettability state will be changed and the oil droplet turns into Wenzel State,^[47] resulting in the pinning state of oil droplets (Fig. 4f). As the surface is reheated to a temperature higher than the T_g of ESMP, the polymer is softened and the chain mobility is activated significantly (Fig. 4c), confirmed by the decrease of storage modulus with about 195 times (Fig. S10). In this case, due to the spontaneous release of trapping entropy, the chains will turn to the highest entropy state (Fig. 4d). Accordingly, the permanent pillars' shape with an upright state will exhibit again following the cool of the surface down to room temperature. Due to pillars' shape recovery and constant surface chemical composition (Fig. S17 and Table S1), the underwater low adhesive property can also return. Since the microstructure shape can be reversibly changed based on the shape memory effect of the material, as

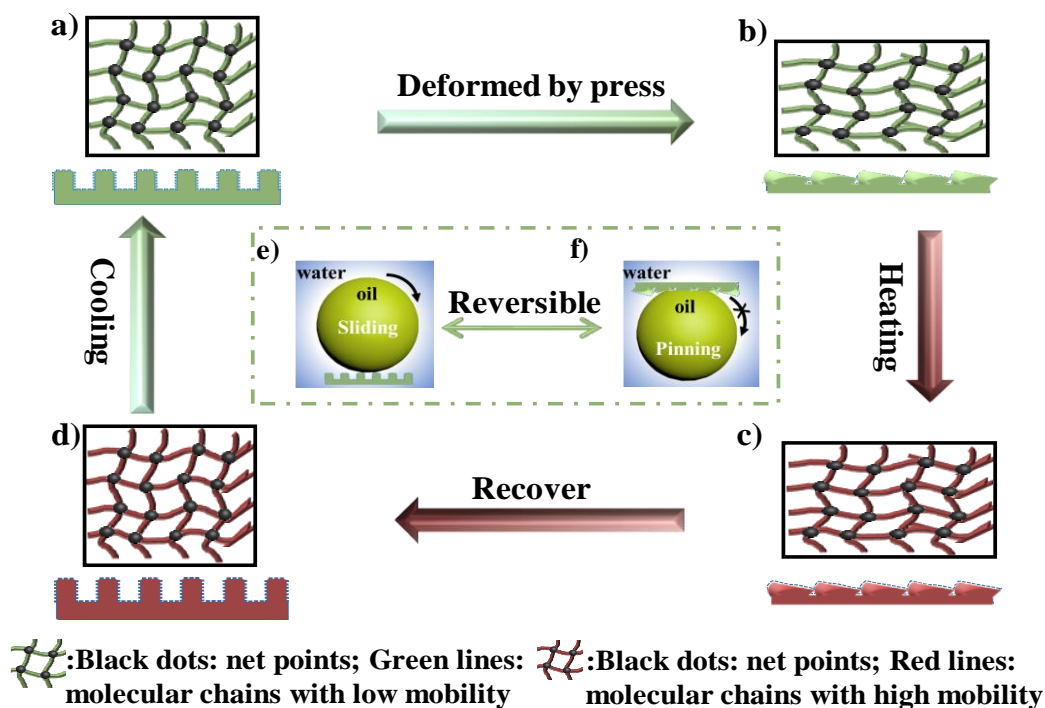


Fig. 4 Schematic diagram of the self-healing process. a) The as-prepared samples are permanent in shape, whose pillars are upright, containing the highest entropy due to the conformation of the molecular chains and lots of crossing linking networks. b) The pillars are pressed by an external force, on which process the slippage of the long-range chain was prohibited by crosslinking networks, forming a new chain conformation with lower entropy. c) The surface with a temporary shape is heated and the molecular chain was activated. d) The surface with recovery micro/nano morphology with the highest entropy, due to the release of stored energy and the recovery of the deformed molecular chains based on the thermodynamically favorable tendency for increasing entropy. e) and f) are surfaces with upright and collapsed pillars showing superoleophobicity with low and high adhesion underwater, according to Cassie state and Wenzel state.

demonstrated in Fig. 3b, the surface superoleophobicity between low adhesion and high adhesion can be repeatedly controlled by cycled pressing/recovery processes.

The obtained self-healing surface can simultaneously display a special adhesion transition of oil droplets in water between the rolling state and pinning state, which has a huge potential in a lot of applications, for example, as the smart droplet control platform and microdroplet-related functional patterned chips. As is well known, similar super wetting platforms and functional chips have demonstrated wide applications in cell adhesion/transfection,^[48,49] drug delivery,^[50] and controlled droplet transportation^[51,52] arousing much attention in various fields. However, those reported works, including our previous work to prepare patterned surfaces,^[35] selective capture/release of microdroplets,^[38] and platforms for reversible gradient wetting property^[33] or reversible directional transportation,^[36] almost all those reports are focused on droplet manipulation in air through morphological^[53,54] or chemical control.^[55] Therefore, it is still hard to get a similar functional chip and programmable oil droplet storage in water. Herein, based on the as-prepared self-healing surface, these imperfections can be conquered easily. As shown in Fig. 5a, the surface pattern (such as “H”) can be achieved by pressing the surface with a template under a temperature higher than T_g of ESMP. Based on the special oil droplet adhesion underwater, the patterned surface can be employed as a memory chip for oil droplets. Meanwhile, due to the shape memory effect of the ESMP substrate, the as-prepared surface can be re-programmed after removing the pattern “H” by heating and constructing the

pattern of “I” and “T” successively, finally achieving the programmable storage of oil droplets in water. In addition, the surface with various pillar states can also be used for the transportation of oil droplets underwater. As demonstrated in Fig. 5b, an oil droplet is positioned at the surface of the upright pillar with low adhesion initially. Then the droplet will go to the surface with collapsed pillars when letting it close to the droplet gradually due to the higher adhesion on collapsed surfaces. Similarly, when a higher adhesion surface, such as the smooth ESMP surface, is utilized to contact the oil droplet again, it will be transported into the smooth ESMP surface, completing the whole process of transportation.

4. Conclusions

In summary, new underwater superoleophobic and low adhesive surfaces with the capacity for self-healing crushed micromorphology and wettability were reported in this work. The surfaces were obtained by constructing hierarchical micro/nanostructure with ESMP material through template transfer method and modifying by APTES. When the hierarchical micro/nanostructure was destroyed, the underwater low adhesion property of oil droplets could be easily repaired via a simple heating process, owing to the superior shape memory effect of the employed polymer material. Besides, relying on the difference of underwater adhesion, the achieved surfaces could be used in oil droplet storage and transportation in water. Moreover, we report a new strategy for designing self-healing underwater

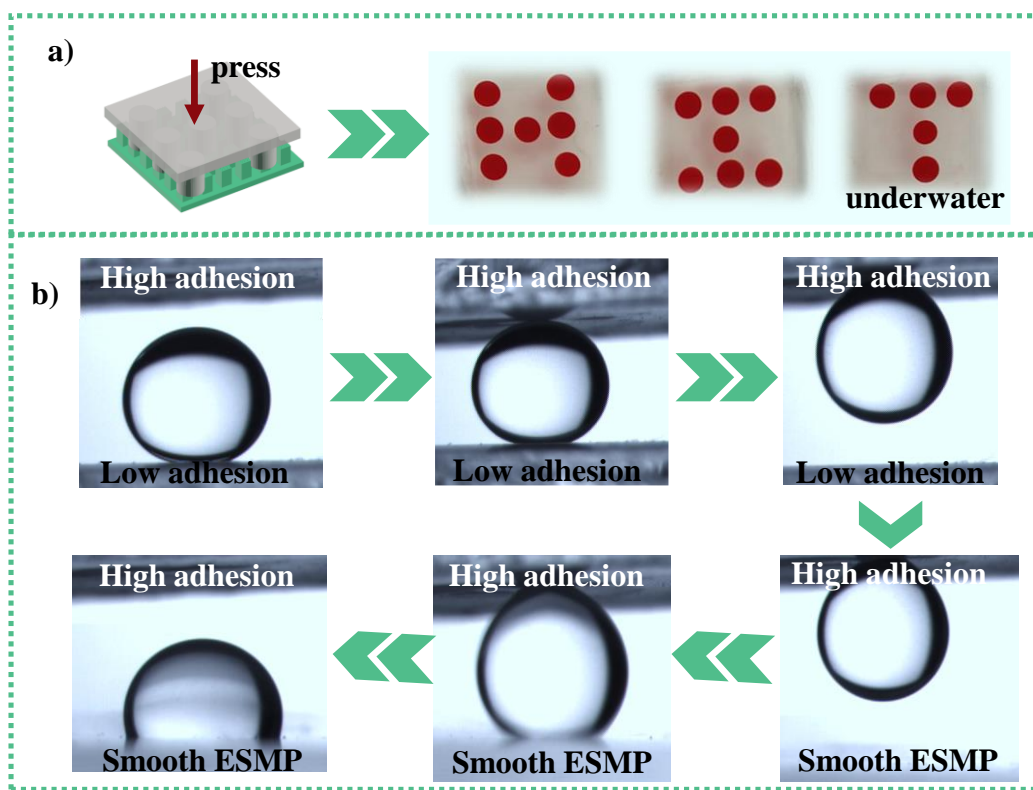


Fig. 5 Applications of as-obtained surfaces as a reversible storage platform for oil droplets in water media (a) and transportation of the oil droplet (b).

superoleophobic materials by applying the ESMP. The strategy is simple and thermal-responsive shape memory polymer is just used as an example. It is rational to believe that the strategy can be easy to extend to many other shape memory materials that are responsive to other stimuli such as light, magnetic field, and electricity.

Acknowledgments

This work was supported by the National Natural Science Foundation of China (NSFC Grant No. 22075061 and 51573035), Funding of Key Laboratory of Bioinspired Materials and Interfacial Science, TIPC, CAS, Postdoctoral innovative talent support program (No. BX20200106), China Postdoctoral Science Foundation (No. 2020M681106), and Heilongjiang Postdoctoral Fund (No. LBH-Z20149).

Conflict of interest

There are no conflicts to declare.

Supporting information

Applicable.

References

- [1] S. Zarghami, T. Mohammadi, M. Sadrzadeh, B. Van der Bruggen, *Progress in Polymer Science*, 2019, **98**, 101166, doi: 10.1016/j.progpolymsci.2019.101166.
- [2] K. Liu, Y. Tian, L. Jiang, *Progress in Materials Science*, 2013, **58**, 503-564, doi: 10.1016/j.pmatsci.2012.11.001.
- [3] J. Yong, F. Chen, Q. Yang, Z. Jiang, X. Hou, *Advanced Materials Interfaces*, 2018, **5**, 1701370, doi: 10.1002/admi.201701370.
- [4] T. Jiang, Z. Guo, W. Liu, *Journal of Materials Chemistry A*, 2015, **3**, 1811-1827, doi: 10.1039/c0xx00000x.
- [5] Y. Zhao, X. Yang, L. Yan, Y. Bai, S. Li, P. Sorokin, L. Shao, *Journal of Membrane Science*, 2021, **618**, 118525, doi: 10.1016/j.memsci.2020.118525.
- [6] L. Qiu, Y. Sun, Z. Guo, *Journal of Materials Chemistry A*, 2020, **8**, 16831-16853, doi: 10.1039/x0xx00000x.
- [7] Z. Li, Z. Guo, *Nanoscale*, 2019, **11**, 22636-22663, doi: 10.1039/c9nr05870b.
- [8] S. Zhang, G. Jiang, S. Gao, H. Jin, Y. Zhu, F. Zhang, J. Jin, *ACS Nano*, 2018, **12**, 795-803, doi: 10.1021/acsnano.7b08121.
- [9] J. Huang, Q. Wang, Z. Wu, Z. Ma, C. Yan, Y. Shi, B. Su, *Advanced Functional Materials*, 2021, **31**, 2103776, doi: 10.1002/adfm.202103776.
- [10] C. Wang, F. Zhang, C. Yu, S. Wang, *ACS Applied Materials & Interfaces*, 2020, **12**, 42430-42436, doi: 10.1021/acsaami.0c12573.
- [11] W. Liu, S. Xiang, X. Liu, B. Yang, *ACS Nano*, 2020, **14**, 9166-9175, doi: 10.1021/acsnano.0c04670.
- [12] J. Ge, D. Zong, Q. Jin, J. Yu, B. Ding, *Advanced Functional Materials*, 2018, **28**, 1705051, doi: 10.1002/adfm.201705051.
- [13] D. Wang, Q. Sun, M. J. Hokkanen, C. Zhang, F.-Y. Lin, Q. Liu, S.-P. Zhu, T. Zhou, Q. Chang, B. He, Q. Zhou, L. Chen, Z. Wang, R. H. A. Ras, X. Deng, *Nature*, 2020, **582**, 55-59, doi: 10.1038/s41586-020-2331-8.
- [14] L. Lin, H. Yi, X. Guo, P. Zhang, L. Chen, D. Hao, S. Wang, M. Liu, L. Jiang, *Science China Chemistry*, 2018, **61**, 64-70, doi: 10.1007/s11426-017-9149-x.
- [15] C. Neinhuis, K. Koch, W. Barthlott, *Planta*, 2001, **213**, 427-434, doi: 10.1007/s004250100530.
- [16] T.-S. Wong, S. H. Kang, S. K. Y. Tang, E. J. Smythe, B. D. Hatton, A. Grinthal, J. Aizenberg, *Nature*, 2011, **477**, 443-447, doi: 10.1038/nature10447.
- [17] W. Chen, P. Zhang, R. Zang, J. Fan, S. Wang, B. Wang, J. Meng, *Advanced Materials*, 2020, **32**, 1907413, doi: 10.1002/adma.201907413.
- [18] C. Long, Y. Qing, K. An, C. Liu, M. Chai, C. Yang, C. Liu, *Chemical Engineering Journal*, 2020, **385**, 123920, doi: 10.1016/j.cej.2019.123920.
- [19] D. Parbat, U. Manna, *Chemical Science*, 2017, **8**, 6092-6102, doi: 10.1039/c7sc01055a.
- [20] C. Li, H. Lai, Z. Cheng, J. Yan, M. An, *Nanoscale*, 2018, **10**, 20435-20442, doi: 10.1039/c8nr05173a.
- [21] M. Wu, Y. Li, N. An, J. Sun, *Advanced Functional Materials*, 2016, **26**, 6777-6784, doi: 10.1002/adfm.201601979.
- [22] S. Xiang, W. Liu, *Advanced Materials Interfaces*, 2021, **8**, 2100247, doi: 10.1002/admi.202100247.
- [23] S. Fu, H. Zhou, H. Wang, H. Niu, W. Yang, H. Shao, T. Lin, *Materials Horizons*, 2019, **6**, 122-129, doi: 10.1039/c8mh00898a.
- [24] Y. Wang, Y. Liu, J. Li, L. Chen, S. Huang, X. Tian, *Chemical Engineering Journal*, 2020, **390**, 124311, doi: 10.1016/j.cej.2020.124311.
- [25] Y. Li, L. Li, J. Sun, *Angewandte Chemie*, 2010, **49**, 6129-6133, doi: 10.1002/ange.201001258.
- [26] H. Wang, Y. Xue, J. Ding, L. Feng, X. Wang, T. Lin, *Angewandte Chemie International Edition*, 2011, **50**, 11433-11436, doi: 10.1002/anie.201105069.
- [27] M. Ge, C. Cao, F. Liang, R. Liu, Y. Zhang, W. Zhang, T. Zhu, B. Yi, Y. Tang, Y. Lai, *Nanoscale Horizons*, 2020, **5**, 65-73, doi: 10.1039/c9nh00519f.
- [28] K. Chen, S. Zhou, L. Wu, *Chem Commun*, 2014, **50**, 1189-11894, doi: 10.1039/c3cc49251f.
- [29] D. Wang, H. Liu, J. Yang, S. Zhou, *ACS Applied Materials & Interfaces*, 2019, **11**, 1353-1362, doi: 10.1021/acsaami.8b16464.
- [30] K. Chen, S. Zhou, L. Wu, *ACS Nano*, 2016, **10**, 1386-1394, doi: 10.1021/acsnano.5b06816.
- [31] W. Wang, J. Salazar, H. Vahabi, A. Joshi-Imre, W. E. Voit, A. K. Kota, *Advanced Materials*, 2017, **29**, 1700295, doi: 10.1002/adma.201700295.
- [32] L. Zhao, J. Zhao, Y. Liu, Y. Guo, L. Zhang, Z. Chen, H. Zhang, Z. Zhang, *Small*, 2016, **12**, 3327-3333, doi: 10.1002/smll.201600092.
- [33] D. Zhang, Z. Cheng, H. Kang, J. Yu, Y. Liu, L. Jiang, *Angewandte Chemie International Edition*, 2018, **57**, 3701-3705, doi: 10.1002/anie.201800416.
- [34] Z. Cheng, D. Zhang, X. Luo, H. Lai, Y. Liu, L. Jiang, *Advanced Materials*, 2021, **33**, 2001718, doi: 10.1002/adma.202001718.
- [35] H. Zhang, H. Lai, Z. Cheng, D. Zhang, P. Liu, Y. Li, Y. Liu,

- Applied Surface Science*, 2020, **525**, 146525, doi: 10.1016/j.apsusc.2020.146525.
- [36] Z. Cheng, D. Zhang, T. Lv, H. Lai, E. Zhang, H. Kang, Y. Wang, P. Liu, Y. Liu, Y. Du, S. Dou, L. Jiang, *Advanced Functional Materials*, 2018, **28**, 1705002, doi: 10.1002/adfm.201705002.
- [37] J. K. Park, S. Kim, *Lab on a Chip*, 2017, **17**, 1793-1801, doi: 10.1039/c6lc01354f.
- [38] Y. Wang, H. Lai, Z. Cheng, H. Zhang, Y. Liu, L. Jiang, *ACS Applied Materials & Interfaces*, 2019, **11**, 10988-10997, doi: 10.1021/acsami.9b00278.
- [39] J. Song, M. Gao, C. Zhao, Y. Lu, L. Huang, X. Liu, C. J. Carmalt, X. Deng, I. P. Parkin, *ACS Nano*, 2017, **11**, 9259-9267, doi: 10.1021/acsnano.7b04494.
- [40] T. Lv, Z. Cheng, E. Zhang, H. Kang, Y. Liu, L. Jiang, *Small*, 2017, **13**, 1503402, doi: 10.1002/smll.201503402.
- [41] H. Qian, D. Xu, C. Du, D. Zhang, X. Li, L. Huang, L. Deng, Y. Tu, J. M. C. Mol, H. A. Terry, *Journal of Materials Chemistry A*, 2017, **5**, 2355-2364, doi: 10.1039/c6ta10903a.
- [42] T. Lv, Z. Cheng, D. Zhang, E. Zhang, Q. Zhao, Y. Liu, L. Jiang, *ACS Nano*, 2016, **10**, 9379-9386, doi: 10.1021/acsnano.6b04257.
- [43] Y. Peng, Y. Ning, X. Ma, Y. Zhu, S. Yang, B. Su, K. Liu, L. Jiang, *Advanced Functional Materials*, 2018, **28**, 1800712, doi: 10.1002/adfm.201800712.
- [44] T. Xie, *Polymer*, 2011, **52**, 4985-5000, doi: 10.1016/j.polymer.2011.08.003.
- [45] J. Puig, I. A. Zucchi, C. E. Hoppe, C. J. Pérez, M. J. Galante, R. J. J. Williams, C. Rodríguez-Abreu, *Macromolecules*, 2009, **42**, 9344-9350, doi: 10.1021/ma9018203.
- [46] A. B. D. Cassie, S. Baxter, *Transactions of the Faraday Society*, 1944, **40**, 546, doi: 10.1039/tf9444000546.
- [47] R. N. Wenzel, *Industrial & Engineering Chemistry*, 1936, **28**, 988-994, doi: 10.1021/ie50320a024.
- [48] L. Chen, M. Liu, H. Bai, P. Chen, F. Xia, D. Han, L. Jiang, *Journal of the American Chemical Society*, 2009, **131**, 10467-10472, doi: 10.1021/ja9019935.
- [49] R. Sheparovych, M. Motornov, S. Minko, *Advanced Materials*, 2009, **21**, 1840-1844, doi: 10.1002/adma.200802449.
- [50] S. T. Yohe, Y. L. Colson, M. W. Grinstaff, *Journal of the American Chemical Society*, 2012, **134**, 2016-2019, doi: 10.1021/ja211148a.
- [51] C. Li, C. Yu, D. Hao, L. Wu, Z. Dong, L. Jiang, *Advanced Functional Materials*, 2018, **28**, 1707490, doi: 10.1002/adfm.201707490.
- [52] K. Han, L. Heng, Y. Zhang, Y. Liu, L. Jiang, *Advanced Science*, 2019, **6**, 1801231, doi: 10.1002/advs.201801231.
- [53] D. Tian, N. Zhang, X. Zheng, G. Hou, Y. Tian, Y. Du, L. Jiang, S. X. Dou, *ACS Nano*, 2016, **10**, 6220-6226, doi: 10.1021/acsnano.6b02318.
- [54] J. Wang, L. Sun, M. Zou, W. Gao, C. Liu, L. Shang, Z. Gu, Y. Zhao, *Science Advances*, 2017, **3**, e1700004, doi: 10.1126/sciadv.1700004.
- [55] H. Li, W. Fang, Z. Zhao, A. Li, Z. Li, M. Li, Q. Li, X. Feng, Y. Song, *Angewandte Chemie International Edition*, 2020, **59**,

Author Information



Dongjie Zhang is currently a postdoctor at Harbin Institute of Technology. She received her B.S. degree (2014) in polymer materials and engineering and Ph.D. (2020) in chemical engineering and technology from Harbin Institute of Technology. From 2018 to 2019, she was a visiting student at Mark Maclachlan group in the University of British Columbia, Canada. Her present research interest is focused on smart materials, such as shape memory polymers, materials with controllable wettability.



Zhongjun Cheng obtained his B.S. (2003) and M.S. (2006) degrees in chemistry from Jilin University in Jilin, P.R. China, and his Ph.D. (2009) from the Institute of Chemistry, Chinese Academy of Science in Beijing, under the supervision of Professor Lei Jiang. He is currently Associate Professor at Harbin Institute of Technology in Heilongjiang, P.R. China. His scientific interest is in the design and fabrication of superwetting materials with dynamic tunable micro-/nanostructures, and related applications.



Yuyan Liu obtained her B.S. and PhD in department of polymer materials and engineering at Harbin Institute of Technology in Harbin in China. Since 1998, she has been working as a lecturer in Harbin Institute of Technology. During 2001 to 2002, she went to University of Tokyo as a visiting scholar in Japan. Since 2006, she became a professor in Harbin Institute of Technology. Her research interests cover construction and intelligent control of micro/nano structure on polymer surface, spatial flexible rigid materials, shape memory polymer and composite materials, recycling of polymer materials.

Publisher's Note: Engineered Science Publisher remains neutral with regard to jurisdictional claims in published maps and institutional affiliations.